A Green Method for Synthesis of Silver-Nanoparticles-Diatomite (AgNPs-D) Composite from Pineapple (*Ananas comosus*) Leaf Extract

Saprini Hamdiani[1,2] and Yeng-Fong Shih[1*]

[1]*Department of Applied Chemistry, Chaoyang University of Technology, No. 168, Jifeng E. Rd., Wufeng District, Taichung 41349, Taiwan*

[2]*Department of Chemistry, Faculty of Mathematics and Natural Sciences, University of Mataram, Jl. Majapahit No.62, NTB 83115, Indonesia*

* ***Corresponding author:***

tel: +04-23323000 ex 4308, 7272
email: syf@cyut.edu.tw

Received: January 25, 2021
Accepted: March 15, 2021

DOI: 10.22146/ijc.63573

Abstract: *This study aims to develop a green method to load silver nanoparticles (AgNPs) into the diatomite (D) pores to produce AgNPs-D composite material. The AgNPs were synthesized by pineapple leaf extract at the temperature of 70 °C for 30 min. The composite formation was characterized by UV-Vis, FTIR, TGA, particle sizes analysis, gravimetric, and color observation. The appearance of surface plasmon bands in 440–460 nm confirms the AgNPs formation. The percentage of the $AgNO_3$ which converted to AgNPs was 99.8%. The smallest particle size of AgNPs was 30 nm, obtained in an $AgNO_3$ concentration of 1 mM with a stirring time of 24 h at 70 °C. The colloidal AgNPs were stable for up to 7 days. The adsorption process of AgNPs was marked by the appearance of –C=O and –C–O– groups peak at 1740 and 1366 cm^{-1} on the FTIR spectrum. By adsorption and gravimetric technique, as much as 1 wt.% of AgNPs were loaded into D pores. The color of diatomite material changes from white to reddish-brown. The TGA analysis showed that the remaining D and AgNPs-D at 580 °C are 98.22% and 95.74%, respectively. The AgNPs loading through the green technology technique was expected to increase diatomite application in the biomedical field.*

Keywords: *pineapple leaf extract; diatomite; silver nanoparticles; green method*

■ INTRODUCTION

Diatomite is an inorganic material naturally formed from fossilized single-celled aquatic algae called diatomite [1]. The main diatomite composition is SiO_2; other components include Al_2O_3, Fe_2O, CaO, MgO, and other organics [2]. The material's physical properties are lightweight, low density, thermal conductivity, high porosity, and surface area, inertness, and high absorption capacity [3-4]. The composition and excellent physical properties make diatomite potential for application as a filler of composite material in industrial and biomedical applications [5].

In the industrial field, diatomite is applied as a filler in many applications such as for the adsorption of dye materials [6], separation of oil from crude oil [7], sensors [8], catalyst support, thermal storage [9], and pollution prevention of heavy metals in drinking water [10]. In the biomedical field, diatomite is applied as a drug delivery material [11], biosensing [12], a filler for making scaffold and bone tissue regeneration [13]. As a filler for scaffold and bone tissue regeneration, diatomite is used for reinforced porous polyurethane foam (PUF) [14] and chitosan composite membrane [15]. The addition of diatomite increases the mechanical strength and water uptake capacity of the polymer. Another biomedical application for diatomite is a precursor for leusite synthesis. Leusite is an essential material in Porcelain-Fused-to-Metal (PFM) and all-ceramic restoration systems. This material produces transparency, depth of color, and texture of natural teeth [16]. However, the use of diatomite in the biomedical field is limited because it does not contain antibacterial properties. The large porosity of diatomite makes antibacterial substrate easy to load into the diatomite pores. Diatomite, as matrix

minerals for antibacterial carrier agents, is a promising economic material.

One of the elements that possessed excellent antibacterial properties is silver nanoparticles (AgNPs). The substances are not toxic to humans but have high toxicity to microorganisms such as bacteria, viruses, and fungi [17-19]. The resulting silver nanoparticles (AgNPs) will be loaded into the diatomite (D) pores to obtain silver-nanoparticle diatomite (AgNPs-D) composite material. Several methods were used to load silver nanoparticles into the diatomite pores. Chen et al. (2020) have used the Ag^+ adsorption method from an electrolytic cell and calcination in high temperatures of 500 and 800 °C [20]. Qi et al. (2020) fabricated silver-diatomite nanocomposite ceramic with silver nitrate adsorption by diatomite. The composite was then added with a carboxymethyl cellulose solution followed by calcination at 400 °C [21]. Besides, the researchers used chemicals such as sodium borohydride solution [22], hydrogen peroxide [23], and Tollens' reagent [24-25] to produce AgNPs. However, some of these methods are not environmentally friendly and expensive because they use high calcination temperatures and toxic reducing agents.

The environmentally friendly, non-toxic, safe, and low-cost method to produce AgNPs-D composites is necessary to develop. The method used is synthesized silver nanoparticles using the leaf extract from agricultural waste [26-27]. One of the ample abundances of agricultural waste in Taiwan is pineapple (*Ananas comosus* L) leaf. Every year, more than 5 million tons of pineapple leaf trash are produced [28]. The phytochemical content in the leaf extract acts both as a reducing and capping agent for the formation of AgNPs [29-30]. The phytochemical compound in the pineapple leaf extract includes terpenoids, flavonoids, cardiac glycosides, phytosterols, alkaloids, and saponins [31], causing the reduction process of Ag^+ to Ag^0. The reduction process is then followed by stabilization to form stable oligomeric clusters of silver nanoparticles. The AgNPs are loaded into the diatomite pores by the adsorption process. Adsorption is an effective and efficient method for loading metal nanoparticles into the pores of porous materials [32]. The resulting silver nanoparticle-diatomite (AgNPs-D) composite will potentially be applied as a filler in the biomedical field.

■ EXPERIMENTAL SECTION

Materials

Pineapple leaf was collected from the pineapple plantation area in Wufeng District, Taiwan, $AgNO_3$ (Sigma–Aldrich chemicals), and diatomite (Cellite® 577; density = 0.47 g/cm^3, content: 80~90% SiO_2, 2~4% Al_2O_3, and 0.5~2% Fe_2O_3) was supplied by Imerys Filtration Minerals Inc.

Instrumentation

FTIR (Perkin Elmer Two Spectrum, USA), UV-Visible Spectrophotometer (Perkin Elmer PDA UV-Vis, Lambda 265, USA), Laser particle sizer (Fritsch Analysette 22), and TA Instruments TGA Q50 thermogravimetric analyzer.

Procedure

Preparation of leaf extract

Fresh pineapple leaf was washed and chopped. The leaf was then dried at room temperature and extracted with distilled water. Next, 10 g of the dried leaf was added with 200 mL of distilled water and boiled at 60 °C for 1 h. The mixture was then filtered with no.1 Whatman filter paper. The filtrate was collected and kept at 4 °C and was further used to synthesize the silver nanoparticles.

Synthesis of silver nanoparticles using the pineapple leaf extract

The filtrate (5 mL) of pineapple leaf extract was added to 50 mL of 1 mM, 2 mM, and 3 mM aqueous solution of $AgNO_3$. The solution was heated at 70 °C for 30 min, and the color change was observed. Afterward, the solution was stirred for 4, 8, 24, 28, and 30 h, respectively, at a speed of 800 rpm to complete the nanoparticle formation. The sample was taken for UV-Visible and particle size analysis.

Stability of particle size distribution in silver nanoparticles (AgNPs) solution

Stability of Particle Size Distribution in Silver Nanoparticles (AgNPs) solution: The 1 mM solution of

synthesized AgNPs was stored at the period of 3, 7, 9, 14, 21, and 30 days. At the range of the periods, the distribution of particle size was measured by particle size analysis equipment.

Preparation of AgNPs-D (diatomite, which loaded by AgNPs)

Diatomite was processed to enhance the surface area and total pore volume by the calcination process at 400 °C for 2 h. The diatomite was added to the silver nanoparticles solution at room temperature. It stirred continuously for 8 h to complete the adsorption of AgNPs into the diatomite pores. The mixture was heated at 60 °C for 24 h to remove the solvents, and AgNPs-D powder was obtained.

■ RESULTS AND DISCUSSION

The Phytochemical Compound in Pineapple Leaf Extracts for AgNPs Formation

Collecting the phytochemical compound, such as secondary metabolite in pineapple leaf extract, is carried out by the extraction process in distilled water. Before processing, the pineapple leaves were dried at room temperature. The drying process aims to reduce the presence of water. The reduced water content will create more space for the solvent to penetrate the cells and increase the secondary metabolites extracted from the leaves [33]. Pineapple leaf extract contains secondary metabolites include 13 types of phenolic constituents. There are five major phenolic compounds: cafeic acid, *p*-coumaric acid, 1-O-caffeoylgycerol, 1-O-coumaroylglycerol, and 1,3-O-dicaffeoylglycerol (ananasate) [34-36]. The secondary metabolites of leaf extract play an essential role in reducing and capping silver nanoparticle formation. Carbonyl and hydroxyl functional groups found in the pineapple leaf extract forces the reduction process. The groups as a reduction agent and stabilize the nanoparticles by preventing aggregation [37]. The reduction and stabilization process occurs in one single step:

$$AgNO_3 \rightarrow Ag^+ + NO_3^-$$

$$Ag^+ + \text{Leaf extracts} \rightarrow Ag^0$$

Illustration of reduction and stabilization of silver nanoparticles by the phytochemical compound in pineapple leaf extract shown in Fig. 1. The nanoparticle formation occurred in 3 steps. The steps are reduction, nucleation, and crystal growth. Reduction occurs because the carbonyl and hydroxyl groups have a higher redox potential than other groups and become the electron source that transfers to metal [38]. The reduction process causes the beginning of crystal nanoparticle formation (nucleation). During the process of crystal formation completed, the carbonyl and hydroxyl will stabilize the nanoparticle crystals formed.

UV-Visible Spectroscopy

The formation of silver nanoparticles was detected by UV-Visible Spectroscopy analysis shown in Fig. 2. The characteristic plasmon band for silver nanoparticle formation was ranging between 440–460 nm (a). The peak appears due to the reduction of Ag^+ to Ag^0, the nucleation process, and the complete crystal growth process. Completing the crystal growth process is characterized by a change in the $AgNO_3$ solution color of the reddish-brown [39]. The color change is caused by the excitation process and changes in electronic energy on the surface plasmon band vibrations due to silver nanoparticle formation. In general, free electrons in metals vibrate after being exposed to UV light. Electron vibrations resonate with light waves, resulting in the highest absorption characteristic at the peak of 425 nm.

Particle Size Analysis

In this study, the synthesis of AgNPs involves the heating process at a temperature of 70 °C for 30 min. The heat treatment affects the formation and average diameter of AgNPs. According to research conducted by Hongyu Liu et al. (2020), the particle size of AgNPs is smaller at the temperature of 70 °C than between 75–90 °C [40]. A static laser light scattering technique conducted distribution and particle size measurement. The method can cover a particle measuring range from approximately ten nanometers up to a few millimeters. The particle size distribution of the AgNPs in the variation of concentration and stirring time is shown in Table 1.

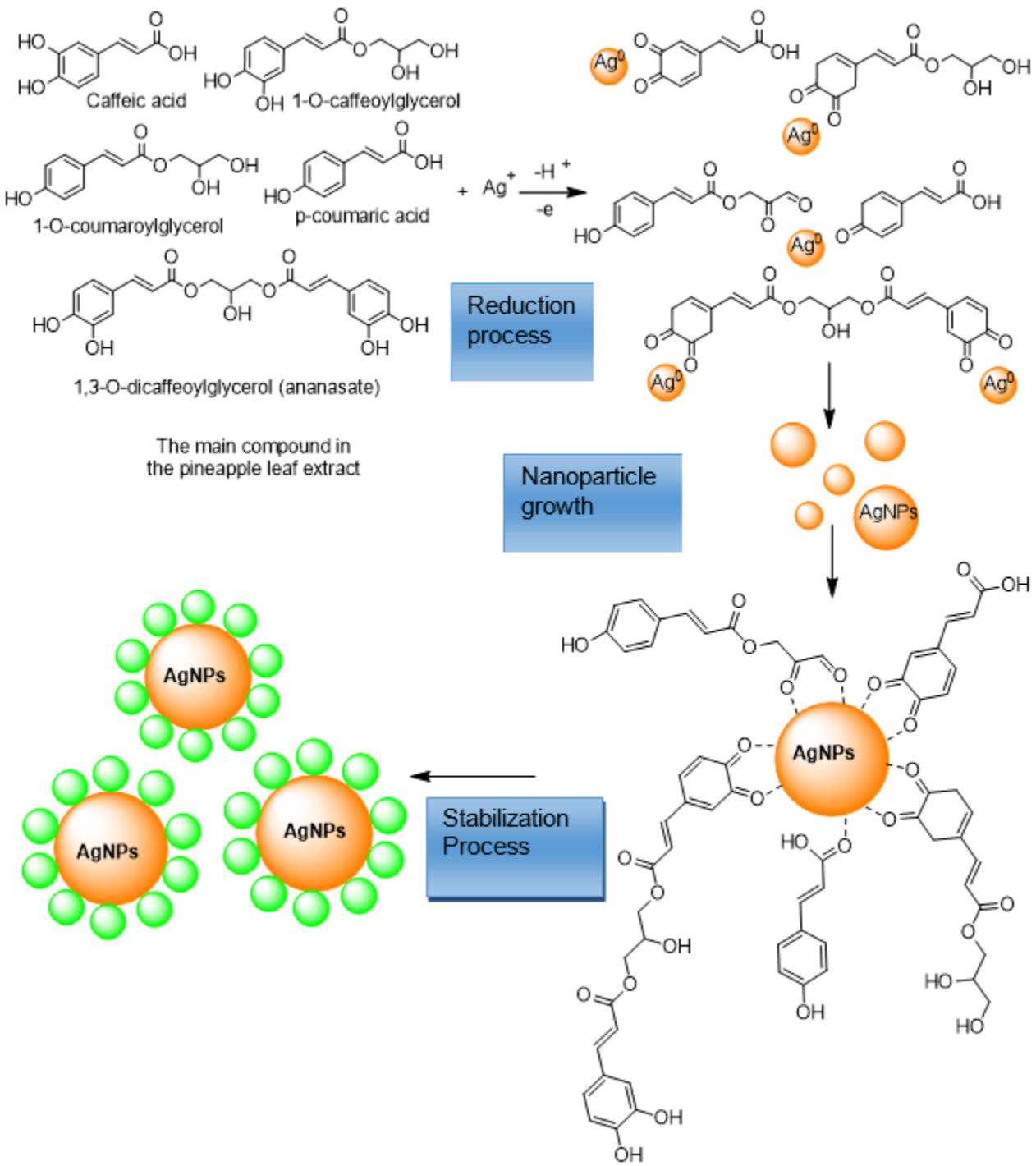

Fig 1. Illustration of silver nanoparticle formation and stabilization by the phytochemical compounds in the pineapple leaf extract

Table 1 shown that heat treatment and stirring time also affect the particle size and distribution of nanoparticles [41]. For AgNPs 1 mM, the variation of stirring time of 4, 8, 16, and 24 h affected the percentage, mean, and median values of AgNPs. At 16 and 24 h, the nanoparticle formation percentages were 99.5% and 99.8%. The smallest mean and median values were obtained during the stirring process for 24 h. At the

higher AgNPs concentrations (2 and 3 mM), the longer stirring times of 28 and 30 h were required for AgNPs formation. The histogram of the particle size distribution is shown in Fig. 3.

Stability of Particle Size Distribution of AgNPs Solution

The stability of AgNPs in the solution was determined by measuring changes in particle size with different storage times. The stabilities of the AgNPs in the leaf extract lasted in 7 days. At the storage time of 9, 14, 21, and 30 days, the particle sizes of AgNPs became more than 100 nm. The increase of nanoparticle sizes in solution, influenced by pH, ionic strength, the formation of Ag_2O, and electrolyte type [42]. In the synthesis of nanoparticles using leaf extracts, a longer storage time will increase the amount of Ag^+ species. The Ag^+ ion released then forms a black precipitate which is most likely Ag_2O. This can be seen from the darker color of the solution and the formation of black deposits in the AgNPs solution

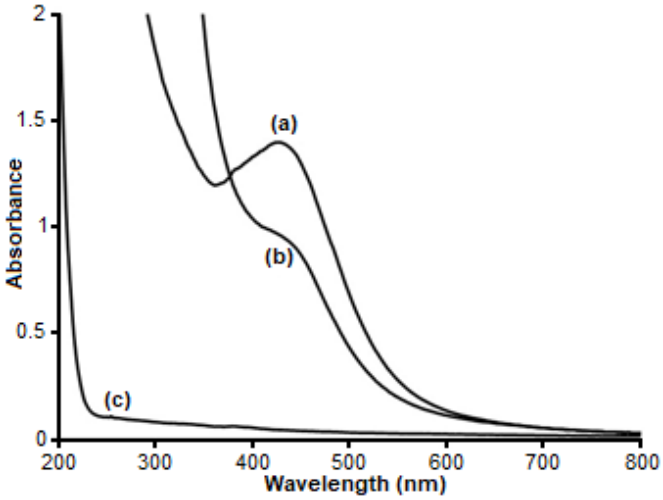

Fig 2. UV-Visible spectra of: (a) AgNPs, (b) Pineapple leaf extract, (c) $AgNO_3$ solution

Table 1. The particle size distribution of silver nanoparticle in variation $AgNO_3$ concentration and stirring time

[$AgNO_3$] (mM)	T (°C)	Total stirring time (h)	Particle size (nm)	%	Mean (nm)	Median (nm)
1	70	4	< 100	89.1	350	50
			101–200	7.2		
			> 300	3.7		
1	70	8	< 100	93.4	300	30
			101–200	4.3		
			> 300	2.3		
1	70	16	< 100	99.5	100	20
			101–200	0.2		
			> 300	0.3		
1	70	24	< 100	99.8	30	20
			101–200	0.2		
			300	0		
2	70	4	< 100	83.6	92	50
			101–200	9.0		
			>300	7.4		
2	70	28	< 100	98.3	70	30
			101–200	1.1		
			> 300	0.6		
3	70	4	< 100	0.3	11730	641
			101–200	17.8		
			> 300	81.9		
3	70	30	< 100	99.4	50	20
			101–200	0.4		
			> 300	0.2		

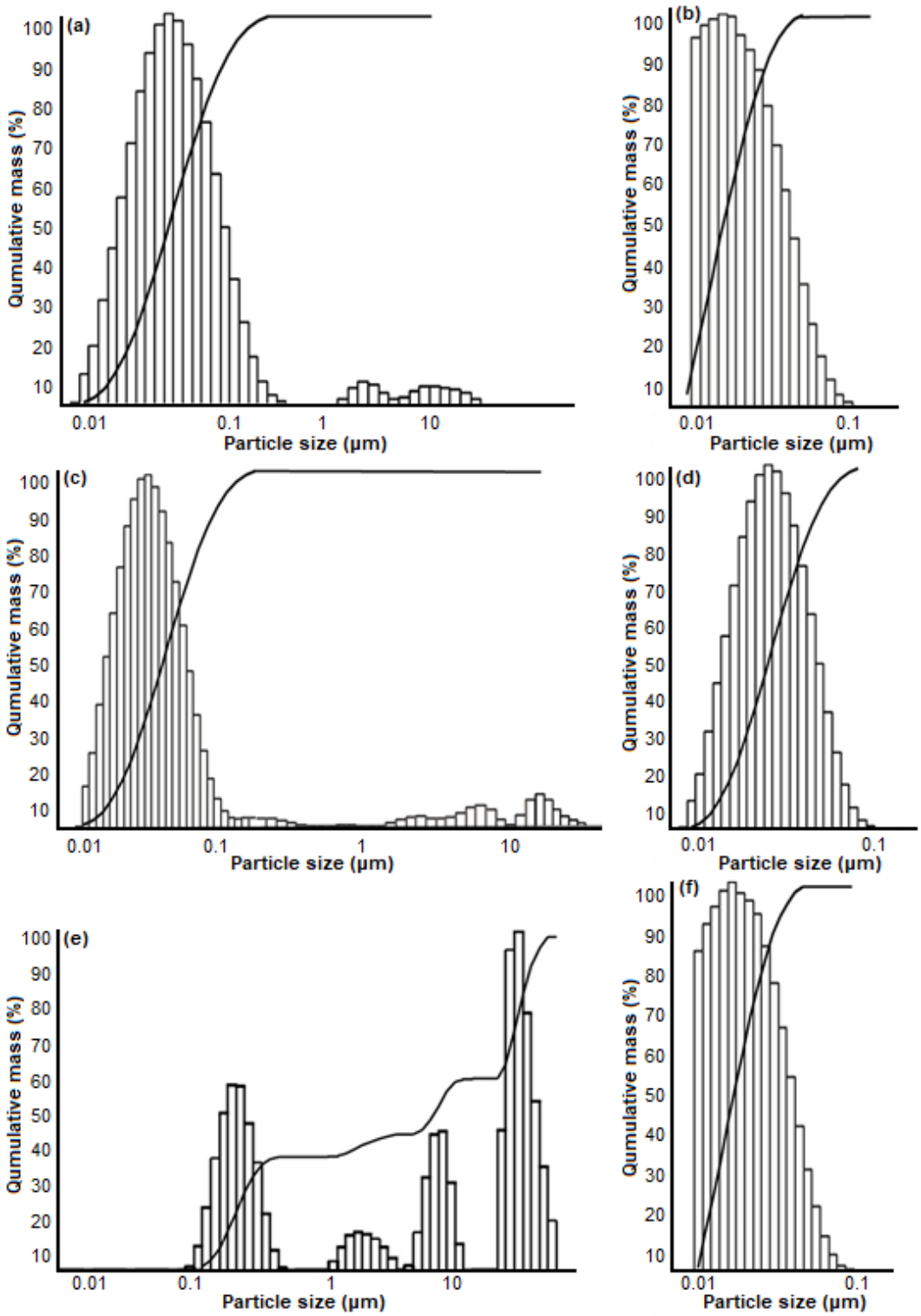

Fig 3. Histogram of the particle size distribution in (a) 1 mM AgNPs, stirred for 4 h and (b) 24 h, (c) 2 mM AgNPs, stirred for 4 h and (d) 28 h, (e) 3 mM AgNPs, stirred for 4 h and (f) 30 h

stored for more than 7 days. The formation of Ag_2O increases the particle sizes of nanoparticles [43]. The formation of the darker color of the solution is shown in Fig. 4. The particle size distribution of the AgNPs 1 mM

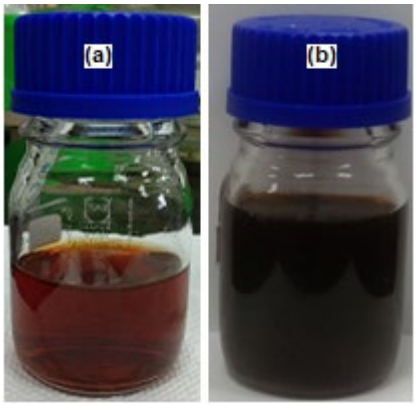

Fig 4. AgNPs solution after (a) 24 h and (b) 30 days

with variations in storage time is shown in Table 2 and Fig. 5.

FTIR Spectroscopy for AgNPs

Fig. 6. exhibits FTIR spectra of pineapple leaf extract (a) shows the broad peak at 3369 cm^{-1} could be assigned to O–H stretch, while the peaks at 2972, 1375, and 1218 cm^{-1} could be attributed to C–H stretching vibration. The peak at 1375 and 1218 cm^{-1} could be identified as –C–O single bond absorption. The adsorption band at 1722 and 1641 cm^{-1} could be identified as –C=O carbonyl and –C=C stretching of the cyclic aromatic ring. These peaks correspond to the functional groups of five major compounds found in the pineapple leaf extract. Fig. 6(b) showed the spectra of the AgNPs. The shift in wavenumbers for the functional groups –OH, –C=O and the increase in the –C–O groups transmittance because these functional groups affect the reduction and stabilization processes in forming AgNPs. The presence of the AgNPs influenced the additional peaks at 1596, 1039, and 770 cm^{-1} [44-46]. A few characteristic peaks of pineapple leaf extract were exhibited in AgNPs. The work observed that AgNPs still contain organic material from pineapple leaf extract.

Silver Nanoparticles Loaded on Diatomite (AgNPs-D)

An adsorption process carried out the loaded process of AgNPs into the diatomite pore. Diatomite was heated at 400 °C for 2 h to maximize the adsorption of AgNPs. According to research by Shih et al. (2020), the heating process to diatomite waste at 400 °C increases the surface area and pore volume [47]. The percentage of AgNPs loaded into the diatomite pore was measured using a gravimetric technique. The technique is based on the weighing process before and after adsorption to determine

Table 2. The particle size of 1 mM of AgNPs in the storage time variation

No.	Storage time (day)	Particle size (nm)	%	Mean	Median
1	3	< 100	99.8	30.0 nm	20.0 nm
		101–200	0.2		
		> 100	-		
2	7	< 100	99.8	30.0 nm	20.0 nm
		101–200	0.2		
		> 100	-		
3	9	< 100	-	5.36 µm	5.34 µm
		101–200	-		
		> 100	100		
4	14	< 100	-	377.4 µm	373.4 µm
		101–200	-		
		> 100	100		
5	21	< 100	-	534.3 µm	532.5 µm
		101–200	-		
		> 100	100		
6	30	< 100	-	754.8 µm	746.69 µm
		101–200	-		
		> 100	100		

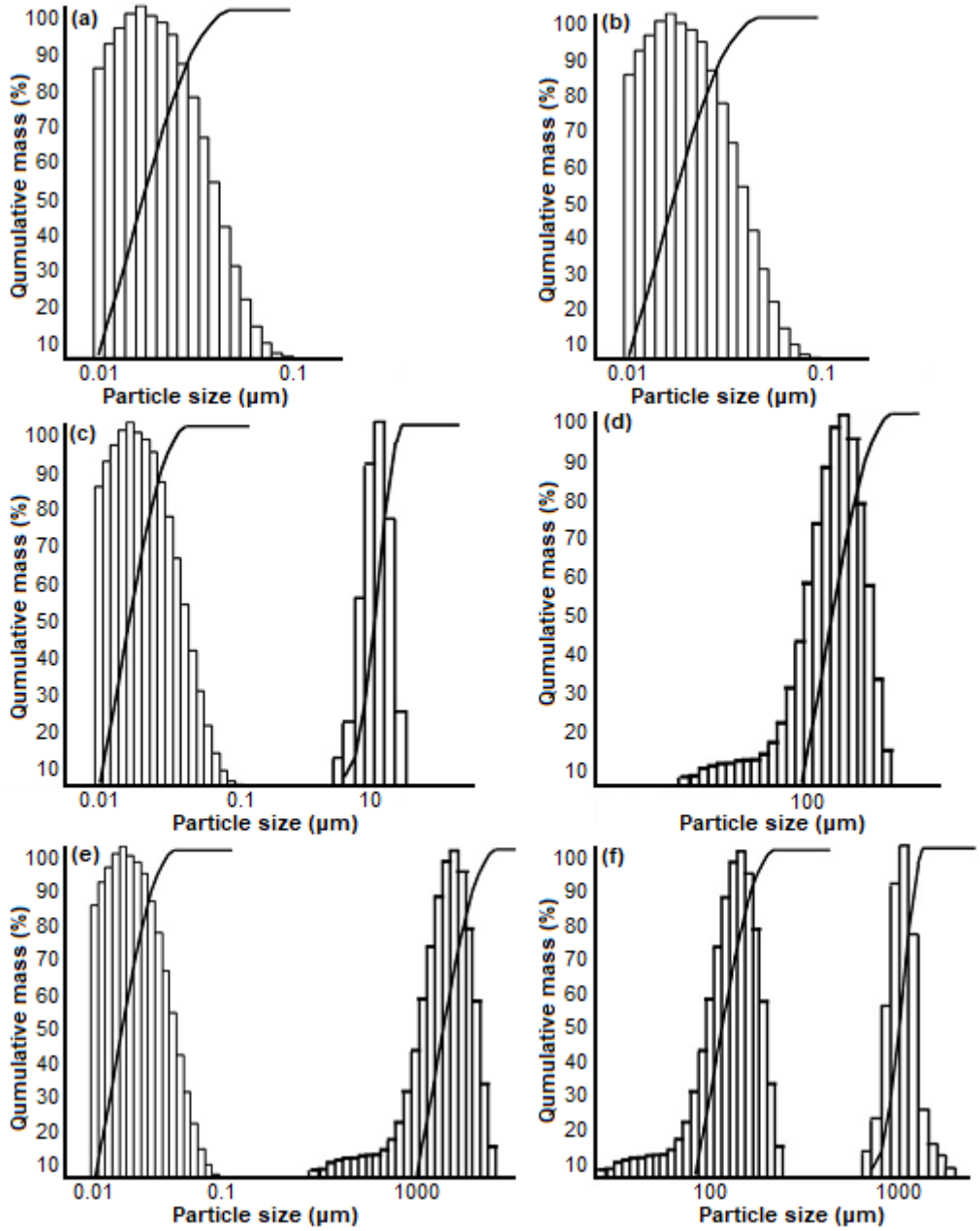

Fig 5. Histogram of the particle size distribution of 1 mM AgNPs stored for (a) 3, (b) 7, (c) 9, (d) 14, (e) 21, and (f) 30 days

the amount of AgNPs loaded into the diatomite pores.

In this study, as much as 1 wt.% of silver nanoparticles were loaded into the diatomite pores. Based on the gravimetric analysis, the initial weight of diatomite (w_o) was 0.8692 g. The adsorption of AgNPs into diatomite pores produces AgNPs-D. The AgNPs-D composite was then dried and heated at 200 °C. The drying and heating process of AgNPs-D composites resulted in the final weight (w_f) = 0.8792 g. The weight increased of AgNPs-D was 1 wt.%, indicating that 1% of AgNPs was successfully loaded in the diatomite pores. The loading of AgNPs into the diatomite pores was also evidenced by the change in the diatomite color from white to reddish-brown (the characteristic color of AgNPs), as shown in Fig. 7. FTIR spectra of diatomite and AgNPs-D are demonstrated in Fig.8.

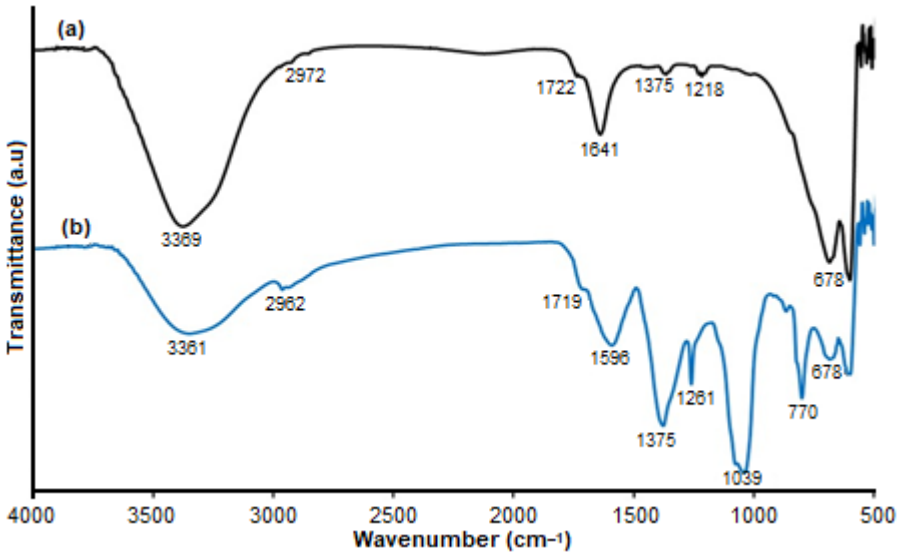

Fig 6. FTIR spectra of (a) pineapple leaf extract and (b) AgNPs

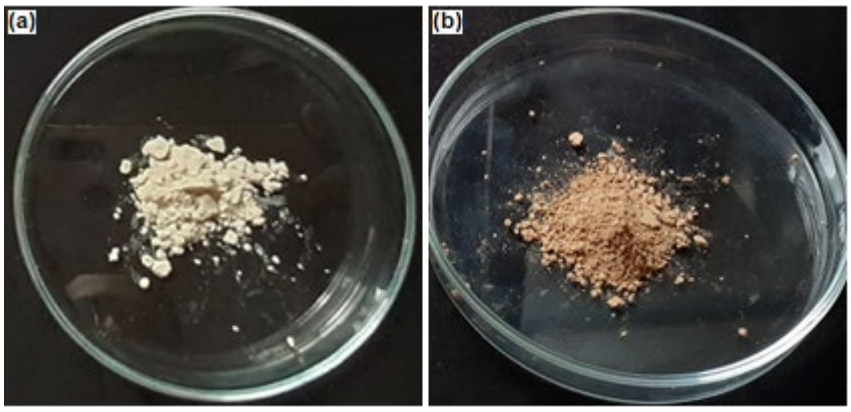

Fig 7. (a) Diatomite, (b) AgNPs-D composite

Fig. 8(b) shows the FTIR spectra for AgNPs-D. The characteristic peaks indicated the loaded AgNPs into the diatomite pores are observed at 1740 and 1366 cm^{-1}, attributable to the -C=O groups and C–H stretching vibration. This absorption indicates that the AgNPs loaded into the diatomite pores still contain organic compounds from pineapple leaf extract. The wavenumber shifts for the Si–O–Si and Si–O groups from 1088 to 1090 cm^{-1} and 803 to 799 cm^{-1} caused by the entry of AgNPs into the diatomite pores.

Thermal Analysis of Diatomite and AgNPs-D

Diatomite is a potential filler to enhance the thermal properties of the composite material. Thermal analysis (TGA) was performed to determine the effect of AgNPs on the thermal resistance of AgNPs-D. TGA thermogram of D and AgNPs-D are shown in Fig. 9. The remaining material measured by thermal analysis for D and AgNPs-D were 98.22 and 95.74%, respectively. The organic compounds in AgNPs cause the remaining material to be reduced compared to D. The insertion of AgNPs to D was successfully proved by the organic compound found in AgNPs-D. In D and AgNPs-D material, weight loss occurs in the range of 100–580 °C. At a temperature of 100-200 °C, the decrease in weight due to the loss of water molecules. In the next phase, the reduction in the weight percentage of D and AgNPs-D occurred at temperatures of 141–430 °C and 142–450 °C. The decrease was caused by the decomposition of organic matter. Based on Kristl (2015), organic matter

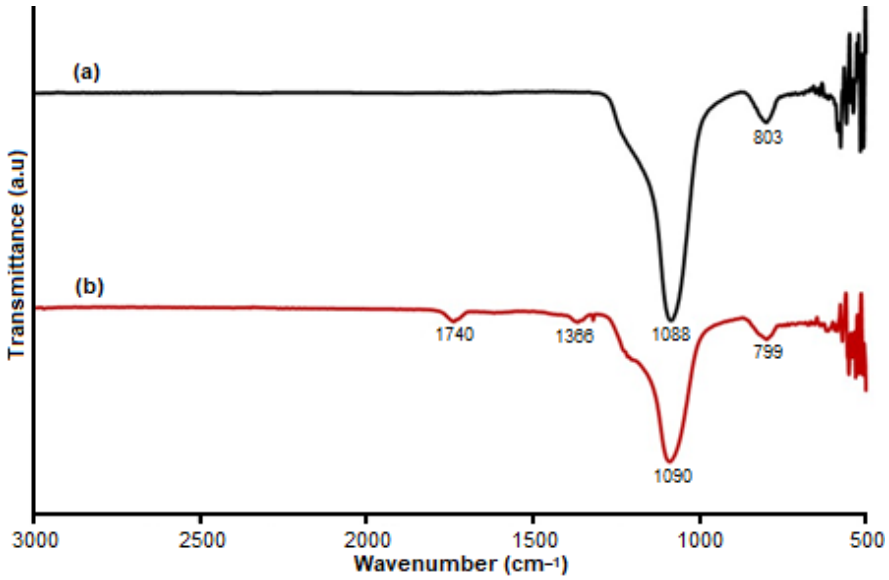

Fig 8. FTIR spectra of (a) Diatomite and (b) AgNPs-D

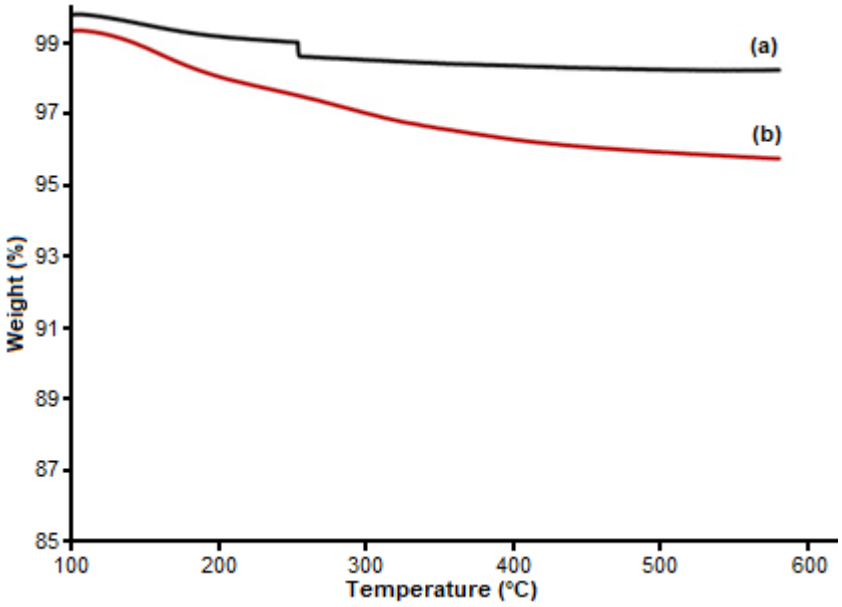

Fig 9. TGA Thermogram of (a) D, (b) AgNPs-D

decomposition will begin at a temperature of 180–450 °C [48]. Besides, the weight loss percentage is not caused by the breakdown of diatomites minerals because the process takes place at temperatures above 650 °C [49].

■ CONCLUSION

Research has been conducted on developing a green method to prepare AgNPs from pineapple leaf extract loaded on diatomite pores. The results showed that the pineapple leaf extract plays an essential role in converting the 99.8% $AgNO_3$ solution into AgNPs. The size distribution of the AgNPs was affected by the temperature and the total stirring time. The smallest mean and median values for AgNPs 1 mM were 30 and 20 nm, obtained after the stirring time for 24 h. The stability of the AgNPs solution lasts for seven days. The particle size was more than 100 nm after seven days of storage. After one month of storage, the particle size was recorded as 754.8 μm (mean) and 746.69 μm (median). The successful loading of AgNPs into D exhibited by

gravimetric techniques, as much as 1 wt.% of AgNPs, was loaded into diatomite pores. The diatomite changes color to reddish-brown. The appearance of the peak for –C=O and –C–O– groups at 1719 and 1375 cm^{-1} indicates that AgNPs still contain organic compounds from pineapple leaf extract. The TGA analysis showed that the residual material D and AgNPs-D were 98.22% and 95.74% at 580 °C. The AgNPs loaded to diatomite pores will improve the performance of the material as an antibacterial agent. The properties will expand the applications of AgNPs-D composites in the biomedical and industrial fields.

■ AUTHOR CONTRIBUTIONS

Conceptualization of the presented idea, S. Hamdiani (Saprini Hamdiani) and Y.F. Shih (Yeng-Fong Shih); methodology, S. Hamdiani, and Y.F. Shih; fabricated the sample and data curation, S. Hamdiani; writing—original draft preparation, S. Hamdiani, and Y.F. Shih; writing–review and editing, S. Hamdiani and Y.F. Shih. All authors have read and agreed to the published version of the manuscript.

■ REFERENCES

[1] Lutyński, M., Sakiewicz, P., and Lutyńska, S., 2019, Characterization of diatomaceous earth and halloysite resources of Poland, *Minerals*, 9 (11), 670.

[2] Pookmanee, P., Wannawek, A., Satienperakul, S., Putharod, R., Laorodphan, N., Sangsrichan, S., and Phanichphant, S., 2016, Characterization of diatomite, leonardite and pumice, *Mater. Sci. Forum*, 872, 211–215.

[3] Galán-Arboledas, R.J., Cotes-Palomino, M.T., Bueno, S., and Martínez-García, C., 2017, Evaluation of spent diatomite incorporation in clay based materials for lightweight bricks processing, *Constr. Build. Mater.*, 144, 327–337.

[4] Yu, H., Li, C., Zhang, K., Tang, Y., Song, Y., and Wang, M., 2020, Preparation and thermophysical performance of diatomite-based composite PCM wallboard for thermal energy storage in buildings, *J. Build. Eng.*, 32, 101753.

[5] Tramontano, C., Chianese, G., Terracciano, M., de Stefano, L., and Rea, I., 2020, Nanostructured biosilica of diatoms: From water world to biomedical applications, *Appl. Sci.*, 10 (19), 6811.

[6] Xia, K., Liu, X., Chen, Z., Fang, L., Du, H., and Zhang, X., 2020, Efficient and sustainable treatment of anionic dye wastewaters using porous cationic diatomite, *J. Taiwan Inst. Chem. Eng.*, 113, 8–15.

[7] Xu, H., Wang, J., and Ren, S., 2019, Removal of oil from a crude oil-in-water emulsion by a magnetically recyclable diatomite demulsifier, *Energy Fuels*, 33 (11), 11574–11583.

[8] Kong, X., Yu, Q., Li, E., Wang, R., Liu, Q., and Wang, A.X., 2018, Diatomite photonic crystals for facile on-chip chromatography and sensing of harmful ingredients from food, *Materials*, 11 (4), 539.

[9] Li, C., Wang, M., Xie, B., Ma, H., and Chen, J., 2020, Enhanced properties of diatomite-based composite phase change materials for thermal energy storage, *Renewable Energy*, 147, 265–274.

[10] Zhao, Y., Tian, G., Duan, X., Liang, X., Meng, J., and Liang, J., 2019, Environmental applications of diatomite minerals in removing heavy metals from water, *Ind. Eng. Chem. Res.*, 58 (27), 11638–11652.

[11] Janićijević, J., Krajišnik, D., Čalija, B., Vasiljević, B.N., Dobričić, V., Daković, A., Antonijević, M.D., and Milić, J., 2015, Modified local diatomite as potential functional drug carrier–A model study for diclofenac sodium, *Int. J. Pharm.*, 496 (2), 466–474.

[12] Shen, Z., Fan, Q., Yu, Q., Wang, R., Wang, H., and Kong, X., 2021, Facile detection of carbendazim in food using TLC-SERS on diatomite thin layer chromatography, *Spectrochim. Acta, Part A*, 247, 119037.

[13] Tamburaci, S., Kimna, C., and Tihminlioglu, F., 2019, Bioactive diatomite and POSS silica cage reinforced chitosan/Na-carboxymethyl cellulose polyelectrolyte scaffolds for hard tissue regeneration, *Mater. Sci. Eng., C*, 100, 196–208.

[14] Mustafov, S.D., Sen, F., and Seydibeyoglu, M.O., 2020, Preparation and characterization of diatomite and hydroxyapatite reinforced porous polyurethane foam biocomposites, *Sci. Rep.*, 10 (1), 13308.

[15] Tamburaci, S., and Tihminlioglu, F., 2017, Diatomite reinforced chitosan composite

membrane as potential scaffold for guided bone regeneration, *Mater. Sci. Eng., C*, 80, 222–231.

[16] Novembre, D., Gimeno, D., and Poe, B., 2019, Synthesis and characterization of leucite using a diatomite precursor, *Sci. Rep*., 9 (1), 10051.

[17] Susanthy, D., Santosa, S.J., and Kunarti, E.S., 2020, Antibacterial activity of silver nanoparticles capped by *p*-aminobenzoic acid on *Escherichia coli* and *Staphylococcus aureus*, *Indones. J. Chem.*, 20 (1), 182–189.

[18] Akinsiku, A.A., Adekoya, J.A., and Dare, E.O., 2021, *Nicotiana tabacum* mediated green synthesis of silver nanoparticles and Ag-Ni nanohybrid: Optical and antimicrobial efficiency, *Indones. J. Chem.*, 21 (1), 179–191.

[19] Uddin, A.K.M.R., Siddique, M.A.B., Rahman, F., Ullah, A.K.M.A., and Khan, R., 2020, *Cocos nucifera* leaf extract mediated green synthesis of silver nanoparticles for enhanced antibacterial activity, *J. Inorg. Organomet. Polym Mater.*, 30 (9), 3305–3316.

[20] Chen, J.X., Zhu, J.Q., Luo, S.Y., and Zhong, X.Y., 2020, A green method to the preparation of the silver-loaded diatomite with enhanced antibacterial properties, *Chem. Pap*., 74 (3), 859–866.

[21] Qi, X., Chen, J., Li, Q., Yang, H., Jiang, H., Deng, Y., Song, Q., and Liang, T., 2020, Antibacterial silver-diatomite nanocomposite ceramic with low silver release, *Water Supply*, 20 (2), 633–643.

[22] Gao, L., Wang, L., Yang, L., Zhao, Y., Shi, N., An, C., Sun, Y., Xie, J., Wang, H., Song, Y., and Ren, Y., 2019, Preparation, characterization and antibacterial activity of silver nanoparticle/graphene oxide/diatomite composite, *Appl. Surf. Sci.*, 484, 628–636.

[23] Kubasheva, Z., Sprynskyy, M., Railean-Plugaru, V., Pomastowski, P., Ospanova, A., and Buszewski, B., 2020, Synthesis and antibacterial activity of (AgCl, Ag)NPs/diatomite hybrid composite, *Materials*, 13 (15), 3409.

[24] Sherief, M.A., El-Bassyouni, G.T., Gamal, A.A., and Esawy, M.A., 2021, Modification of diatom using silver nanoparticle to improve antimicrobial activity, *Mater. Today: Proc.*, 43, 3369–3374.

[25] Sun, H., Wen, X., Zhang, X., Wei, D., Yang, H., Li, C., and Yang, L., 2018, Biocompatible silver nanoparticle-modified natural diatomite with anti-infective property, *J. Nanomater.*, 2018, 7815810.

[26] Nilavukkarasi, M., Vijayakumar, S., and Kumar, S.P., 2020, Biological synthesis and characterization of silver nanoparticles with *Capparis zeylanica* L. leaf extract for potent antimicrobial and anti proliferation efficiency, *Mater. Sci. Energy Technol.*, 3, 371–376.

[27] Thirumagal, N., and Jeyakumari, A.P., 2020, Structural, optical and antibacterial properties of green synthesized silver nanoparticles (AgNPs) using *Justicia adhatoda* L. leaf extract, *J. Cluster Sci.*, 31 (2), 487–497.

[28] Shih, Y.F., Chou, M.Y., Chang, W.C., Lian, H.Y., and Chen, C.M., 2017, Completely biodegradable composites reinforced by the cellulose nanofibers of pineapple leaves modified by eco-friendly methods, *J. Polym. Res*., 24 (11), 209.

[29] Alsultani, A.M., 2017, *Conocarpus erectus* leaf extract for green synthesis of silver nanoparticles, *Indones. J. Chem.*, 17 (3), 407–414.

[30] Emeka, E.E., Ojiefoh, O.C., Aleruchi, C., Hassan, L.A., Christiana, O.M., Rebecca, M., Dare, E.O., and Temitope, A.E., 2014, Evaluation of antibacterial activities of silver nanoparticles green-synthesized using pineapple leaf (*Ananas comosus*), *Micron*, 57, 1–5.

[31] Hartati, R., Suarantika, F., and Fidrianny, I., 2020, Overview of phytochemical compounds and pharmacological activities of *Ananas Comosus* L., Merr., *Int. J. Res. Pharm. Sci.*, 11 (3), 4760–4766.

[32] Miftiyati, S.D., Hamdiani, S., and Darmayanti, M.G., 2018, Synthesis of paramagnetic merkapto silica hybrid from rice husk ash for Ag(I) adsorbent, *Acta Chim. Asiana*, 1 (2), 30–36.

[33] Justine, V.T., Mustafa, M., Kankara, S.S., and Go, R., 2019, Effect of drying methods and extraction solvents on phenolic antioxidants and antioxidant activity of *Scurrula ferruginea* (Jack) Danser (Loranthaceae) leaf extracts, *Sains Malays.*, 48 (7), 1383–1393.

[34] Ma, C., Xiao, S., Li, Z., Wang, W., and Du, L., 2007, Characterization of active phenolic components in the ethanolic extract of *Ananas comosus* L. leaves using high-performance liquid chromatography with diode array detection and tandem mass spectrometry, *J. Chromatogr. A*, 1165 (1-2), 39–44.

[35] Xie, W., Wang, W., Su, H., Xing, D., Cai, G., and Du, L., 2007, Hypolipidemic mechanisms of *Ananas comosus* L. leaves in mice: Different from fibrates but similar to statins, *J. Pharmacol. Sci.*, 103 (3), 267–274.

[36] Wang, W., Ding, Y., Xing, D.M., Wang, J.P., and Du, L.J., 2006, Studies on phenolic constituents from leaves of pineapple (*Ananas comosus*), *China J. Chin. Mater. Med.*, 31 (15), 1242–1244.

[37] Aritonang, H.F., Koleangan, H., and Wuntu, A.D., 2019, Synthesis of silver nanoparticles using aqueous extract of medicinal plants' (*Impatiens balsamina* and *Lantana camara*) fresh leaves and analysis of antimicrobial activity, *Int. J. Microbiol.*, 2019, 8642303.

[38] Gomes, J.F., Garcia, A.C., Ferreira, E.B., Pires, C., Oliveira, V.L., Tremiliosi-Filho, G., and Gasparotto, L.H.S., 2015, New insights into the formation mechanism of Ag, Au, and AgAu nanoparticles in aqueous alkaline media: Alkoxides from alcohols, aldehydes, and ketones as universal reducing agents, *Phys. Chem. Chem. Phys.*, 17 (33), 21683–21693.

[39] Nayak, D., Ashe, S., Rauta, P.R., Kumari, M., and Nayak, B., 2016, Bark extract mediated green synthesis of silver nanoparticles: Evaluation of antimicrobial activity and antiproliferative response against osteosarcoma, *Mater. Sci. Eng., C*, 58, 44–52.

[40] Balavandy, S.K., Shameli, K., Biak, D.R.A., and Abidin, Z.Z., 2014, Stirring time effect of silver nanoparticles prepared in glutathione mediated by green method, *Chem. Cent. J.*, 8 (1), 11.

[41] Liu, H., Zhang, H., Wang, J., and Wei, J., 2020, Effect of temperature on the size of biosynthesized silver nanoparticle: Deep insight into microscopic kinetics analysis, *Arabian J. Chem.*, 13 (1), 1011–1019.

[42] Bélteky, P., Rónavári, A., Igaz, N., Szerencsés, B., Tóth, I.Y., Pfeiffer, I., Kiricsi, M., and Kónya, Z., 2019, Silver nanoparticles: Aggregation behavior in biorelevant conditions and its impact on biological activity, *Int. J. Nanomed.*, 14, 667–687.

[43] Izak-Nau, E., Huk, A., Reidy, B., Uggerud, H., Vadset, M., Eiden, S., Voetz, M., Himly, M., Duschl, A., Dusinska, M., and Lynch, I., 2015, Impact of storage conditions and storage time on silver nanoparticles' physicochemical properties and implications for their biological effects, *RSC Adv.*, 5 (102), 84172–84185.

[44] Halawani, E.M., 2017, Rapid biosynthesis method and characterization of silver nanoparticles using *Zizyphus spina christi* leaf extract and their antibacterial efficacy in therapeutic application, *J. Biomater. Nanobiotechnol.*, 08, 22–35.

[45] Das, G., Patra, J.K., Debnath, T., Ansari, A., and Shin, H.S., 2019, Investigation of antioxidant, antibacterial, antidiabetic, and cytotoxicity potential of silver nanoparticles synthesized using the outer peel extract of *Ananas comosus* (L.), *PLoS One*, 14 (8), e0220950.

[46] Poadang, S., Yongvanich, N., and Phongtongpasuk, S., 2017, Synthesis, characterization, and antibacterial properties of silver nanoparticles prepared from aqueous peel extract of pineapple, *Ananas comosus*, *Chiang Mai Univ. J. Nat. Sci.*, 16 (2), 123–133.

[47] Shih, Y.F., Wang, C.H., Tsai, M.L., and Jehng, J.M., 2020, Shape-stabilized phase change material/nylon composite based on recycled diatomite, *Mater. Chem. Phys.*, 242, 122498.

[48] Kristl, M., Muršec, M., Šuštar, V., and Kristl, J., 2016, Application of thermogravimetric analysis for the evaluation of organic and inorganic carbon contents in agricultural soils, *J. Therm. Anal. Calorim.*, 123 (3), 2139–2147.

[49] Ibrahim, S.S., and Selim, A.Q., 2012, Heat treatment of natural diatomite, *Physicochem. Probl. Miner. Process.*, 48 (2), 413–424.